This article was downloaded by:
On: *14 January 2011*
Access details: *Access Details: Free Access*
Publisher *Taylor & Francis*
Informa Ltd Registered in England and Wales Registered Number: 1072954 Registered office: Mortimer House, 37-41 Mortimer Street, London W1T 3JH, UK

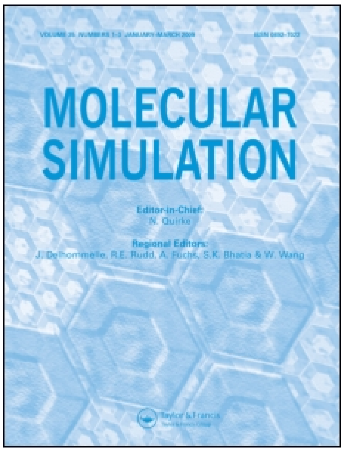

Molecular Simulation
Publication details, including instructions for authors and subscription information:
http://www.informaworld.com/smpp/title~content=t713644482

Two Dimensional Auto-organized Nanostructure Formation of Hyaluronate on Bovine Serum Albumin Monolayer and its Surface Properties

Shouhong Xu; Shizuko Sato; Isamu Miyata; Junpei Yamanaka; Masakatsu Yonese

Online publication date: 13 May 2010

To cite this Article Xu, Shouhong , Sato, Shizuko , Miyata, Isamu , Yamanaka, Junpei and Yonese, Masakatsu(2003) 'Two Dimensional Auto-organized Nanostructure Formation of Hyaluronate on Bovine Serum Albumin Monolayer and its Surface Properties', Molecular Simulation, 29: 10, 711 — 716

To link to this Article: DOI: 10.1080/0892702031000103266

URL: http://dx.doi.org/10.1080/0892702031000103266

PLEASE SCROLL DOWN FOR ARTICLE

Full terms and conditions of use: http://www.informaworld.com/terms-and-conditions-of-access.pdf

This article may be used for research, teaching and private study purposes. Any substantial or systematic reproduction, re-distribution, re-selling, loan or sub-licensing, systematic supply or distribution in any form to anyone is expressly forbidden.

The publisher does not give any warranty express or implied or make any representation that the contents will be complete or accurate or up to date. The accuracy of any instructions, formulae and drug doses should be independently verified with primary sources. The publisher shall not be liable for any loss, actions, claims, proceedings, demand or costs or damages whatsoever or howsoever caused arising directly or indirectly in connection with or arising out of the use of this material.

Molecular Simulation, Vol. 29 (10–11), October–November 2003, pp. 711–716

Taylor & Francis
Taylor & Francis Group

Two Dimensional Auto-organized Nanostructure Formation of Hyaluronate on Bovine Serum Albumin Monolayer and its Surface Properties

SHOUHONG XU*, SHIZUKO SATO, ISAMU MIYATA, JUNPEI YAMANAKA and MASAKATSU YONESE

Faculty of Pharmaceutical Sciences, Nagoya City University, Tanabe-dori Mizuho-ku Nagoya 467-8603, Japan

(Received October 2002; In final form January 2003)

Downloaded At: 18:37 14 January 2011

The layer-by-layer interaction between sodium hyaluronate (NaHA) and bovine serum albumin (BSA) were studied by a quartz crystal microbalance (QCM) method. Their surface structures, adhesive force F_{ad} and frictional behavior were investigated using an atomic force microscope (AFM).

The adsorptions of NaHA on the BSA monolayer were found to be the Langmuir type. The surface structures of NaHA adsorbed on the BSA monolayer were found to form hexagonal-like networks and the mesh size decreased with increasing molecular weight M_w. The F_{ad} between the AFM tip and the surfaces of the saturated NaHA layers increased with increasing value of M_w. However, the frictional coefficient of saturated NaHA layer was found to decrease from 0.933 to 0.191.

Keywords: NaHA; Two dimensional nanostructure; Adhesive force; Friction force

INTRODUCTION

Hyaluronan (HA) is widely distributed in living tissues, not existing alone but usually as proteoglycans (PG) combining with proteins. Its high capacity for holding water and high viscoelasticity give it a unique profile among biological materials and make it suitable for various medical and pharmaceutical applications. Varieties of HA products are found in our daily life. For example, because it retains moisture, HA is used in some cosmetics to keep skin young and fresh-looking. And many ideas for applying HA have been offered in other areas. One of the most successful medical applications is the use of sodium hyaluronate (NaHA) for the treatment of ophthalmology [1–4]. It has also been reported that NaHA was classified by its extensive molecular weight distribution for different applications. For example, the high molar-weight HA could protect the surface of articular cartilage [5], and reduce pain perception [6,7]. As for low molar-weight ones, they could control and normalize the properties of arthritic synovial fluids [8] efficiently. However, the mechanisms and the effect of molecular weight on these medical applications have not yet been fully elucidated. In fact, the effects of HA depending on molecular weight are not clear in various field.

In order to explore the role of HA in articulation or in other body tissues, we have studied the properties of HA and the interactions between HA and proteins not only in solution but also at an interface. The interactions between bovine serum albumin (BSA) and NaHA ($M_w = 850000\,\mathrm{g\,mol^{-1}}$) in solutions have been studied [9,10]. Spherical complexes between NaHA and BSA were formed and the diameters of the particles were controlled by the ratio of BSA to NaHA in the solution. In a previous paper [11], the layer-by-layer interaction between BSA and NaHA ($M_w = 850000\,\mathrm{g\,mol^{-1}}$) were studied and the adsorption of NaHA on the BSA monolayer were found to be the Langmuir type. In this study, in order to understand the effect of molecular weight of NaHA on the surface properties, the layer-by-layer interactions between BSA and various NaHA were studied by quartz crystal microbalance (QCM) method. The surface structures of NaHA layers were observed by using tapping mode atomic force microscope (™AFM). In addition to topographical images, AFM was also employed to probe nanomechanical properties of sample surfaces, such

*Corresponding author.

ISSN 0892-7022 print/ISSN 1029-0435 online © 2003 Taylor & Francis Ltd
DOI: 10.1080/0892702031000103266

Downloaded At: 18:37 14 January 2011

as the local adhesive properties by contact mode. Furthermore, the frictional behaviors were invested by using lateral force microscope (LFM) of AFM and the values of frictional coefficient μ of NaHA layers were estimated.

EXPERIMENTAL

Materials

BSA was purified by delipidizing a BSA Fraction V[10] (Seikagaku kogyou). The average molar weight was determined to be $M_w = 70,000\,\mathrm{g\,mol^{-1}}$ using static light scattering. NaHA were offered from Seikagaku kogyou Co.(Tokyo). Their M_w were 850,000 $\mathrm{g\,mol^{-1}}$ (NaHA85), 210,000 $\mathrm{g\,mol^{-1}}$ (NaHA21) and 23,000 $\mathrm{g\,mol^{-1}}$ (NaHA2.3). Poly(γ-methyl-L-glutamate) PMLG ($M_w = 19,600\,\mathrm{g\,mol^{-1}}$) was also of a commercial origin (SIGMA Co.) and used without any purification.

Preparation of BSA Monolayer on PMLG Cast Film

PMLG cast film was prepared using the same method as mentioned in a previous paper [11]. The tip is denoted by PMLG tip. BSA tip was prepared by immersing the PMLG tip into BSA solution ($C_{BSA}/10^{-6}\,\mathrm{kg\,dm^{-3}} = 10$), in which BSA molecules adsorbed in the saturated state and were confirmed to be a monolayer as shown in our previous paper [11]. The adsorbed amount of BSA in saturated state was $1.3 \times 10^{-6}\,\mathrm{kg\,m^{-2}}$.

Measurement of Adsorption of NaHA on BSA Monolayer using QCM

The adsorbed amounts of NaHA85, NaHA21 and NaHA2.3 on the BSA monolayer were measured by immersing the BSA tip into various concentrations of the NaHA solutions ($C_{NaHA}/10^{-6}\,\mathrm{kg\,dm^{-3}} = 0.5$, 1.0, 2.0, 5.0 and 10, $pH = 6.0$) and the time courses of their adsorptions were determined from the decreases of the resonance frequency of QCM. To reduce the error caused by adsorbed water accompanying adsorption of NaHA molecules, the BSA tip was immersed in water and the frequency in equilibrium was read as an original value before put it into NaHA solutions. Sample solutions were gently stirred in order to avoid the effect of diffusion as much as possible in the condition without losing the stability of the QCM frequency at 25°C.

Analysis of Adsorbed Amounts by QCM

Adsorbed amounts of PMLG, BSA, NaHA85, NaHA21 and NaHA2.3 were obtained using QCM whose resonance frequency is 9 MHz. According to Sauerbrey's equation [12], a frequency decreased of 1 Hz corresponding to a mass increase of 0.87 ng on the QCM electrodes.

Observation of Surface Structures using AFM

Surface structures of the BSA monolayer, and the adsorption layers of NaHA85, NaHA21 and NaHA2.3 were observed by using AFM (Nanoscope III, Digital Instruments Co.). After drying the samples on the QCM tip under the condition of room temperature and atmospheric pressure, the surface structures were observed by a tapping mode in air. An AFM tip was made of Si monocrystal (the spring constant of probe: $33\,\mathrm{N\,m^{-1}}$) and was used without any surface treatment.

Measurement of Adhesive Force using Contact Mode of AFM

Adhesive forces F_{ad} were measured by using contact mode of AFM in solution. The value of F_{ad} between the AFM tips and the sample surfaces were obtained from force curve. The AFM tip was made of Si monocrystal and the normal spring constant K_N given by manufacturer was $0.14\,\mathrm{N\,m^{-1}}$.

Measurement of Friction using Lateral Force Microscope (LFM)

LFM is another function of AFM to obtain friction images of sample surface by a contact mode when scanning an AFM tip in the direction perpendicular to the cantilever. To estimate the frictional force F_f, the torsion signal of the cantilever was recorded when the tip scanned in trace and retrace. The separation between the two curves of the frictional loops gives twice the total frictional signal V. The value of V is relating to the value of ΔX_L (the twisting of the tip of cantilever at the point of contact from the vertical, i.e. the deflection in lateral direction) and S_L (sensitivity of cantilever in lateral direction) as

$$\Delta X_L = V/S_L \tag{1}$$

S_L was also measured by the frictional loops. Then the value of F_f was described by ΔX_L in Eq. (2).

$$F_f = K_L \times \Delta X_L \tag{2}$$

K_L is the cantilever spring constant in lateral direction. The value of K_L can be calculated from normal spring constant K_N according to the formula given by Gibson. For a long-shaped cantilever, the equation is [13]

$$K_L = \frac{2}{3(1+\nu)}\left(\frac{L}{H}\right)^2 K_N \tag{3}$$

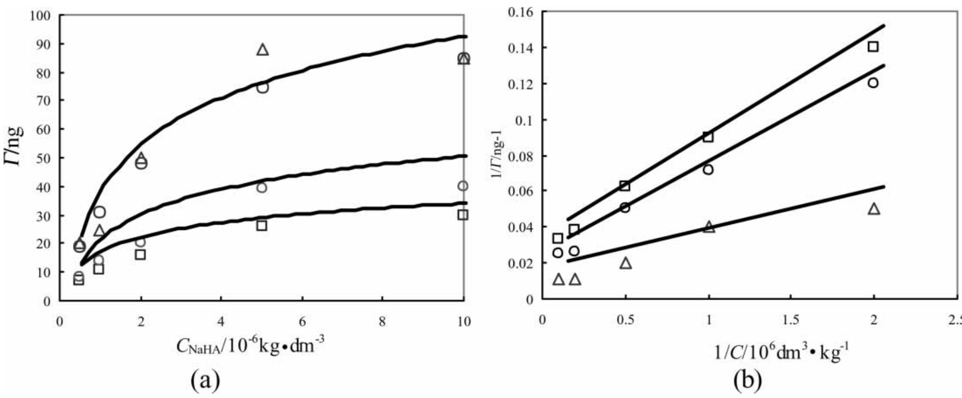

FIGURE 1 (a)Adsorption behavior of NaHA on BSA monolayer. The solid curves show the fitting results calculated from K and Γ^{∞} by Langmuir equation. (b) The reciprocal plots of Γ and C. □: NaHA2.3, ○: NaHA21, △: NaHA85.

Downloaded At: 18:37 14 January 2011

where ν is Poisson ratio which is 0.42 for Si monocrystal, L is the length of the cantilever and the H is the vertical height of tip.

The value of μ between NaHA layers and an AFM tip can be available from Eq. (4).

$$F_{\mathrm{f}} = \mu(F_{\mathrm{load}} + F_{\mathrm{ad}}) \tag{4}$$

F_{load} is a load force exerted by the AFM tip can be given by Eq. (5) [14].

$$F_{\mathrm{load}} = \frac{(A - A_0)K_{\mathrm{N}}}{S_{\mathrm{N}}} \tag{5}$$

where A is the value of setpoint in imaging, A_0 is the value of deflection signal when the tip is in its free state. A_0 and S_{N} were determined by the force curve. In this study F_{ad} was ignored in calculation of F_{f} because the values of F_{ad} were very small compared with those of F_{f}.

RESULTS

Adsorptions of NaHA85, NaHA21 and NaHA2.3 on the BSA Monolayer

As shown in the previous paper[11], the adsorptions of BSA on the PMLG film were Langmuir type and the immobilized BSA molecules were confirmed to adsorb in a monolayer state. The QCM tip covered by PMLG on which BSA is adsorbed in the monolayer state is denoted by BSA tip.

The adsorptions of NaHA85, NaHA21 and NaHA2.3 were measured by immersing the BSA tip in their solutions of various concentrations at 25°C. The time courses of the resonance frequencies F were measured by a QCM. The values of F of the BSA tip decreased and attained constant values with increasing the adsorption. Equilibrium adsorption amounts Γ were obtained from the decreases of the frequencies ΔF at equilibrium states. As shown in Fig. 1(a), the adsorption amounts Γ increased with increasing the concentrations C and showed the Langmuir type adsorptions. The values of Γ of saturated adsorption layers were found to increase with increasing the molar weight of NaHA. The adsorptions were analyzed using the Langmuir's adsorption isotherm [11].

The reciprocal plots of Γ and C are shown in Fig. 1(b). The adsorption constants K and the saturation adsorption amount Γ^{∞} were obtained from the slope of the lines and summarized in Table I with the results of BSA adsorbed on the PMLG film. The value of free energy of adsorption $\Delta G^{\mathrm{o}}_{\mathrm{ads}}$ were also calculated [15] and shown in Table I. The solid curves in Fig. 1(a) showed the fitting results, which were calculated from K and Γ^{∞} by using Langmuir equation. They agreed with the experimental results.

AFM Images of NaHA85, NaHA21 and NaHA2.3 on the BSA Monolayer

After drying the samples under room temperature and atmospheric pressure, surface structures of the saturated adsorption layers of NaHA85, NaHA21 and NaHA2.3 were observed by using AFM in air. Their topographic images are shown by height data in Fig. 2 with BSA monolayer image.

Figure 2(a) shows the surface image of BSA monolayer. Since BSA molecules are very small, it was scanned in a smaller area than those done on

TABLE I Adsorption characteristics of NaHA85, NaHA21 and NaHA2.3 on BSA monolayer

	BSA	*NaHA2.3*	*NaHA21*	*NaHA85*
$(K)/10^6\,\mathrm{dm^3\,kg^{-1}}$	1.35	0.53	0.36	0.45
$(K_{\mathrm{m}})/10^7\,\mathrm{dm^3\,mol^{-1}}$	9.45	38	7.56	1.22
$\Delta G^{\mathrm{o}}_{\mathrm{ads}}/\mathrm{kJ\,mol^{-1}}$	− 45.4	− 49.0	− 44.9	− 40.4
$(\Gamma^{\infty})/10^{-6}\,\mathrm{kg\,m^{-2}}$	1.32	1.04	1.78	3.18
$(\Gamma^{\infty}_{\mathrm{n}})/10^{-8}\,\mathrm{mol\,m^{-2}}$	1.93	4.52	0.85	0.37
n_{HA}		1/2.6	1/22	1/79
n_{re}		26	24	27

K, K_{m}: adsorption constant; $\Delta G^{0}_{\mathrm{ads}}$: free energy of adsorption; Γ^{∞}, $\Gamma^{\infty}_{\mathrm{n}}$: saturated adsorption amount; n_{HA}: the molecular numbers of NaHA on one BSA; n_{re}: repeating unit of NaHA on one BSA.

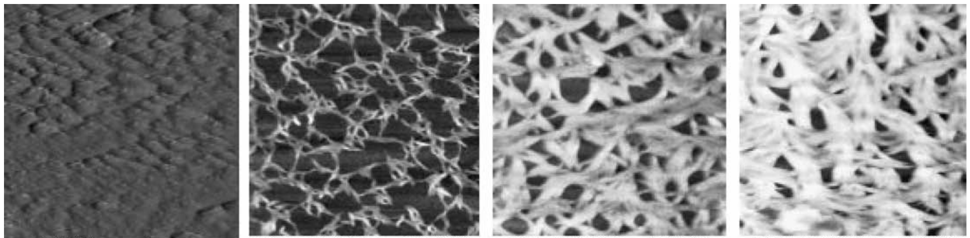

(a) BSAmonolayer (b)NaHA2.3(M_w=230000) (c)NaHA21(M_w=210000) (d)NaHA85(M_w=850000)

FIGURE 2 AFM images of BSA monolayer (1.5 × 1.5 μm) and NaHA in air (5 × 5 μm).

NaHA layers to get a clear image. The roughness of BSA monolayer is 1.1 nm, which was obtained from an offline analysis. Networks structures were found to spread over the BSA monolayer and almost in a hexagonal shape in the image of NaHA2.3. In the images of NaHA21 and NaHA85, the meshes narrowed into very small size and the strands increased in width a lot. The mean sizes of strands were 30–60, 39–150 and 88–150 nm in width and 12, 20 and 32 nm in height estimated from the images, respectively. NaHA molecules are reported to form a double helical structure due to the hydrophobic interaction and the diameters are 2 nm [11]. The strands of network were considered to form by the clusters of NaHA molecules. Then, the numbers of cluster of NaHA molecules composing one strand of the network were estimated from the width and height to be about 90–180 for NaHA2.3, 195–750 for NaHA21 and 700–1200 for NaHA85. It means the number of NaHA clusters constructing the strands of network increased significantly with increasing the molar weight of NaHA. The results indicate that the nanostructure of NaHA layers depend on their molar weights.

Downloaded At: 18:37 14 January 2011

Adhesive Forces of NaHA Layers

The values of F_{ad} between the samples and the AFM tip were measured by the contact mode of AFM in various concentration solutions of NaHA.

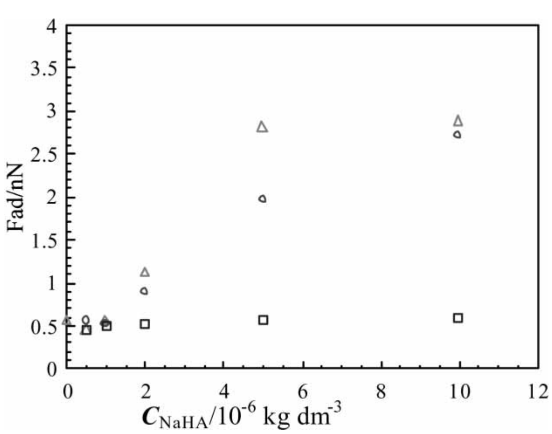

FIGURE 3 Change of adhesive force of BSA monolayer with NaHA adsorption: □: NaHA2.3, ○: NaHA21, △: NaHA85.

The AFM tip was selected soft ones (the spring constant is $0.14\,\mathrm{N\,m^{-1}}$) to be easy to get more accurate data and give less damage to the sample surface.

The values of F_{ad} obtained from force curves were shown in Fig. 3 as a function of C_{NaHA}. The value of F_{ad} increased with increasing the value of C_{NaHA}. In the saturated adsorption NaHA layers, the value of F_{ad} depends on the molecular size of NaHA and increased with increasing the molar weight. The value of F_{ad} at C_{NaHA} being 0 was 0.56 nN, which shows the result of bare BSA monolayer.

Frictional Properties Between NaHA Layers and AFM Tip

The frictional forces between NaHA layer surfaces and AFM tip were measured by using LFM at $2 \times 2\,\mu$m scan area in solution. The same AFM tip was used as mentioned in the measurement of F_{ad}. A lateral signal V could be obtained by the photodiode when scanning the AFM tip on the surface in an angle of 90°. After reading the values of V and the sensitivity of the AFM tip in lateral direction from the friction scope, the value of frictional force could be calculated according to Eqs. (1)–(3). The values of V in various setpoint were recorded for calculation of F_{load}. The relationship between F_f and F_{load} of saturated NaHA layers are shown in Fig. 4. The results were averaged over three or four measurements on different locations of one sample. The values of F_{ad} increased with increasing F_{load}. The plots are linear types and the values of μ of each NaHA layer could be obtained from the slopes of the lines. The values of μ were 0.933, 0.357 and 0.191 for NaHA2.3, NaHA21 and NaHA85, respectively, and found to increase with increasing the molar weight.

DISCUSSION

Formation of Network Structure of NaHA on the BSA Monolayer

The roughness of BSA monolayer was very small (about 1.1 nm) comparing with the thickness of

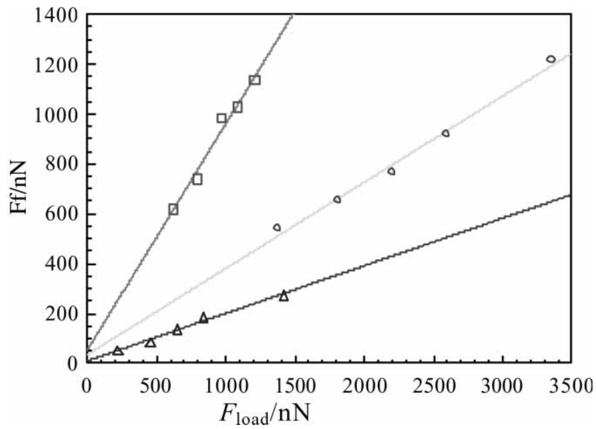

FIGURE 4 The F_f plotted against F_{load} on saturated NaHA layer in various molar weights (C_{NaHA}: $5.0 \times 10^{-6}\,kg\,dm^{-3}$) □: NaHA2.3, ○: NaHA21, △: NaHA85.

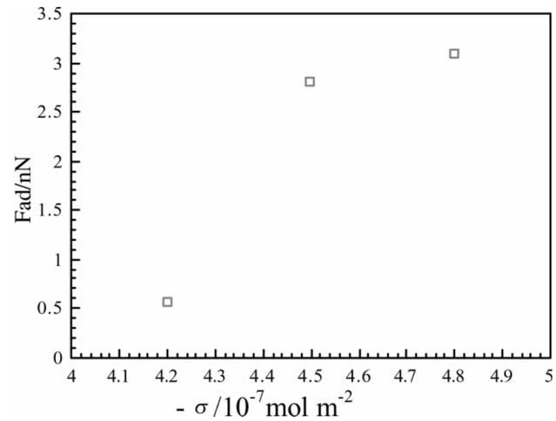

FIGURE 5 F_{ad} ploted against $-\sigma$.

NaHA layers (about 12–32 nm), so it gives little effect on the morphology of NaHA layers. From Fig. 2, the mean values of strands were 12, 20 and 32 nm in height for NaHA2.3, NaHA21 and NaHA85, respectively. Since the diameter of double layers of NaHA was reported to be 2 nm [11], the mean number of NaHA helixes could be estimated to be 6, 10 and 16. Supposing only the lowest layer of NaHA participates in combining with BSA molecules, the values of the molecular numbers n_{HA} and the repeating unit n_{re} of NaHA adsorbed on one BSA molecule were calculated and also shown in Table I.

From the results shown in Table I, the values of n_{HA} were found to depend on the molar weights, i.e. they were 1/2.6 for NaHA2.3, 1/22 for NaHA21 and 1/79 for NaHA85. However, the values of n_{re} were found to be almost constant. The mesh size and structure of NaHA layer were controlled by their molar weight as shown in Fig. 2 (b)–(d). More compact network structure is thought to have more water-holding ability, therefore, higher molar-weight NaHA is advantageous to application in cosmetics to keep the skin moisture.

Adhesive Force of NaHA Layers on BSA Monolyer

The changes of adhesive force due to adsorption of NaHA on BSA monolayer are shown in Fig. 3. The value of F_{ad} of the BSA monolayer increased with increasing the adsorption of NaHA.

It has been proposed that the adhesive forces are closely related to the surface chemical composition, especially to the terminal groups [16,17]. Here, NaHA layer has COO^- terminal groups on the surface. From the images of each NaHA shown in Fig. 2, it is obvious the density of COO^- group depends on molar weight of NaHA. The F_{ad} is affected by the surface charge density σ. Then, in order to understand the relationship between F_{ad} and $-\sigma$ of the saturated NaHA adsorption layer, F_{ad} was plotted against $-\sigma$ in Fig. 5. The values of σ were calculated from the values of Γ_n^∞. From the result, the values of F_{ad} of the saturated adsorption layers were found to increase with increasing the absolute values of $|\sigma|$.

Frictional Coefficient of NaHA Surface in Solution

It is known the value of μ is decided by its surface characteristics such as morphology and surface energy. To clear the relationship between surface morphology and F_f of NaHA layer, the values of mean roughness Ra were obtained by an off-line analysis to be 7.9 nm for NaHA2.3, 10.8 nm for NaHA21 and 11.2 nm for NaHA85. The value of μ was found to decreased with increasing that of Ra. It indicated the F_f was not caused by the morphology of sample surface.

The surface energy increases with increasing F_{ad}. In this study, the values of F_{ad} were very small comparing with that of F_{load} to be ignored in calculation of F_f. Then, the frictional force between NaHA layer surface and AFM tip should be decided by other characteristics of NaHA surface rather than surface morphology and surface energy. These studies should be made progress further more for the application of NaHA in medical and cosmetic region, etc. For example, the NaHA with larger molar weight has more efficacy on reducing friction to protect the surface of cartilage in treatment of osteoarthritis.

From this study, it could be concluded that the surface structure and properties of NaHA layers are controlled by the molar weight. It is necessary to pay more attention to the relationship between molar weight of NaHA and their functions in body tissues.

Downloaded At: 18:37 14 January 2011

Acknowledgements

This research was supported by the grant from Japan Society for the Promotion of Science (JSPS,ID No. P 02183) and the Japan Health Sciences Foundation. Our thanks are extended to Seikagaku Kogyo Co., Ltd. for supplying NaHA samples.

References

[1] Miyauchi, S., Horie, K., Morita, M., Nagahara, M. and Shimizu, K. (1996) "Protective efficacy of sodium hyaluronate on the corneal endothelium against the damage induced by sonication", *J. Ocul. Pharmacol. Ther.* **12**, 27.

[2] Arshinoff, S.A. (1995) "Dispersive and cohesive viscoelastic materials in phacoemulsification", *Ophthal. Practice* **13**, 98.

[3] Asari, A., Morita, M., Sekiguchi, T., Okamura, K., Horie, K. and Miyauchi, S. (1996) "Hyaluronan, CD44 and fibronectin in rabbit corneal epithelial wound healing", *Jpn. J. Ophthalmol.* **40**, 18.

[4] Hassel, J.R., SundarRaj, N., Cintron, C., Midura, R. and Hascall, V.C. (1988) "Alteration in the synthesis of keratan sulfate proteoglycan in corneal wound healing and in macular corneal dystrophy", In: Greiling, H. and Scott, J.E., eds, *Keratan Sulfate*, p 215.

[5] Sakamoto, T., Mizuno, S., Maki, T., Suzuki, T., Yamaguchi, T. and Iwata, H. (1984) "Studies on the affinity of hyaluronic acid to the surface of articular cartilage and the suppression of proteoglycan release from matrix", *Jpn. Orthop. Res. Sci.* **11**, 264.

[6] Gotoh, S., Onaya, J., Abe, M., Miyazaki, K., Hamai, A., Horie, K. and Tokuyasu, K. (1993) "Effects of the molecular weight of hyaluronic acid and its action mechanisms on experimental joint pain in rats", *Ann. Rheum. Dis.* **52**, 817.

[7] Iwata, H. (1993) "Pharmacologic and clinical aspects of intraarticular injection of hyaluronate", *Clin. Orthop.* **289**, 285.

[8] Asari, A., Miyauchi, S., Matsuzaka, S., Ito, T., Kominami, E. and Uchiyama, Y. (1998) "Molecular weight-dependent effects of hyaluronate on the arthritic synovium", *Arch. Histol. Cytol.* **61**, 125.

[9] Yonese, M., Xu, S.H., Kugimiya, S., Sato, S. and Miyata, I. (1997) "Light scattering studies of soluble complexes between hyaluronate and bovine serum albumin", *Prog. Colloid Polym. Sci.* **106**, 252.

[10] Xu, S.H., Yamanaka, J., Sato, S., Miyata, I. and Yonese, M. (2000) "Characteristics of complexes composed of sodium hyaluronate and bovine serum albumin", *Chem. Pharm. Bull.* **48**(6), 779.

[11] Nonogaki, T., Xu, S.H., Kugimiya, S., Sato, S., Miyata, I. and Yonese, M. (2000) "Two dimensional auto-organized nano-structure formation of hyaluronate on bovine serum albumin monolayer and its tension", *Langmuir* **16**, 4272.

[12] Okahata, Y., Kimura, K. and Ariga, K. (1989) "Detection of the phase transition of langmuir- blodgett films on a quartz-crystal microbalance in an aqueous phase", *J. Am. Chem. Soc.* **111**, 9190.

[13] Gibson, C.T., Watson, G.S. and Myhra, S. (1997) "Lateral force microscopy—a quantitative approach", *Wear* **213**, 72.

[14] Li, J., Wang, C., Shang, G., Xu, Q., Lin, Z., Guan, J. and Bai, C. (1999) "Friction coefficients derived from apparent height variations in contact mode atimic force microscopy images", *Langmuir* **15**, 7662.

[15] Kim, C.H., Han, S.W., Ha, T.H. and Kim, K. (1999) "o-Xylene-α, α'-dithiol monolayer film on gold: fourier transform infrared spectroscopy, quartz crystal microbalance, and atomic force microscopy study", 15, 8399.

[16] Chaudhury, M.K. and Whitesides, G.M. (1992) "Correlation between surface free energy and surface constitution", *Science* **255**, 1230.

[17] Feldman, K., Tervoort, T., Smith, P. and Spencer, N.D. (1996) "Toward a force spectroscopy of polymer surface", *Langmuir* **14**, 372.

Downloaded At: 18:37 14 January 2011